

Mitigating the effects of charged particle strikes on TES arrays for exotic atom X-ray experiments

H. Tatsuno¹ · D.A. Bennett² · W.B. Doriese² ·
M. Durkin² · J.W. Fowler² · J.D. Gard² ·
T. Hashimoto³ · R. Hayakawa¹ · T. Hayashi⁴ ·
G.C. Hilton² · Y. Ichinohe⁵ · H. Noda⁶ ·
G.C. O'Neil² · S. Okada⁷ · C.D. Reintsema² ·
D.R. Schmidt² · D.S. Swetz² · J.N. Ullom² ·
S. Yamada¹ · (the J-PARC E62 Collaboration)

the date of receipt and acceptance should be inserted later

Abstract Exotic atom experiments place transition-edge-sensor (TES) microcalorimeter arrays in a high-energy charged particle rich environment. When the high-energy charged particle passes through the silicon substrate of a TES array, a large amount of energy is deposited and small pulses are generated across multiple pixels in the TES array due to thermal crosstalk. We have developed analysis techniques to assess and reduce the effects of charged particle events on exotic atom X-ray measurements. Using of these techniques, the high-energy and low-energy components of the X-ray peaks due to pileup are eliminated, improving energy resolution from 6.6 eV to 5.7 eV at 6.9 keV.

Keywords Transition-edge sensor, Exotic atom, X-ray spectroscopy, Thermal crosstalk, Energy calibration

1 Introduction

Exotic atom X-ray spectroscopy is a unique research technique to investigate the strong interaction between negatively charged particles and nucleus at the low-energy limit. Especially the interaction of kaon (K^-) and nucleus is strongly attractive which shifts and broadens the electromagnetic energy levels of kaonic atom. Therefore, the precision X-ray spectroscopy of kaonic atoms has been performed to determine the strong interaction [1]. We have performed the J-PARC E62 experiment to measure the kaonic helium $3d \rightarrow 2p$ X-rays at the J-PARC K1.8BR beamline (Ibaraki, Japan) [2]. The stopped K^- in the liquid helium

1. Department of Physics, Tokyo Metropolitan University, Tokyo 192-0397, Japan
E-mail: hideyuki.tatsuno@gmail.com
2. National Institute of Standards and Technology, Boulder, CO 80305, USA
3. Japan Atomic Energy Agency (JAEA), Tokai 319-1184, Japan
4. Department of High Energy Astrophysics, Institute of Space and Astronautical Science (ISAS), Japan Aerospace Exploration Agency (JAXA), Kanagawa 229-8510, Japan
5. Department of Physics, Rikkyo University, Tokyo 171-8501, Japan
6. Department of Physics, Osaka University, Osaka 560-0043, Japan
7. Atomic, Molecular and Optical Physics Laboratory, RIKEN, Wako 351-0198, Japan

target forms a kaonic helium atom, then the K^- cascades down to lower energy levels while emitting characteristic X-rays. The X-rays of $3d \rightarrow 2p$ transition (~ 6 keV) are detected with the 240-pixel TES array, which was previously used for pionic atom X-ray spectroscopy [3]. Our goal is to determine the $2p$ -state strong-interaction shift with a precision of 0.2 eV. To achieve this precision, the excellent energy resolution of TES is essential.

The application of TESs at the charged-particle-beam environment requires non-trivial analysis techniques. One of the important analyses is to investigate the charged particle impacts on the TES array. The energy deposits of charged particles on the array, especially on its silicon substrate, can cause small thermal crosstalk pulses in all TESs. The pileup of the thermal crosstalk and normal X-ray pulses degrades the energy resolution due to poor pulse-height estimation via optimal filtering, moreover additional low-energy and high-energy tail components are needed to fit the X-ray peaks [4]. In this paper, we study the effects of charged particle events on the TES array and present analysis methods to improve the energy resolution and the energy calibration for kaonic atom X-ray spectroscopy.

2 Charged particle event identification

We use a group trigger to aid in the identification of thermal crosstalk from charged particle events, a feature recently added to the data acquisition software of the J-PARC E62 experiment [5,6]. In the group trigger, a TES pulse triggers the recording of that TES (primary records) and the four adjacent TESs (secondary records). Fig. 1 (a) shows the primary record of a 6.9 keV Co K_α X-ray event (TES ch 129) that is affected by thermal crosstalk from a charged particle event (id: 654) and one that is not (id: 388), with the difference highlighted in the inset. Fig. 1 (b) shows the secondary records (ch 139, ch 155, ch 161, and ch 171), and Fig. 1 (c) shows the schematic drawing of pixel positions on the array. The thermal crosstalk can be seen in all four adjacent TESs. In this case, the charged particle hit the array 1 ms after the primary X-ray pulse, and the number of charged particle strikes is ~ 40 counts per second per array. Although the pulse height of the thermal crosstalk is less than 1 % of that of Co K_α X-ray, the pulse-shape difference directly affects the pulse-height determination. The electrical crosstalk seen in the TES channel 171 occurs because the channel 129 and 171 are physically nearest neighbors on the multiplexer (MUX) chip. We discuss in the next section how to reduce the influence of this thermal crosstalk.

3 Analysis techniques to reduce the effects of thermal crosstalk

In this section, we discuss the effects of thermal crosstalk on the X-ray energy measurement and techniques to reduce these effects in the analysis process. Due to the use of an optimal filter to determine the pulse height [7,8], the shift of pulse height of an X-ray event is strongly dependent on the arrival time of crosstalk during the record length. If thermal crosstalk arrives during the pre-trigger region (before the X-ray arrival) or in the post peak region (long after the X-ray arrival), the filtered pulse height will be decreased. If the thermal crosstalk arrives during the X-ray pulse peak region (almost the same arrival timing as X-ray), the filtered pulse height will be increased. Depending on the arrival region, the effects of thermal crosstalk from charged particle strikes can be reduced by using event cuts and by reducing record lengths.

Thermal crosstalk in the pre-trigger region is easily identified as deviations from an otherwise constant pre-trigger value in the primary event record. Events affected by the

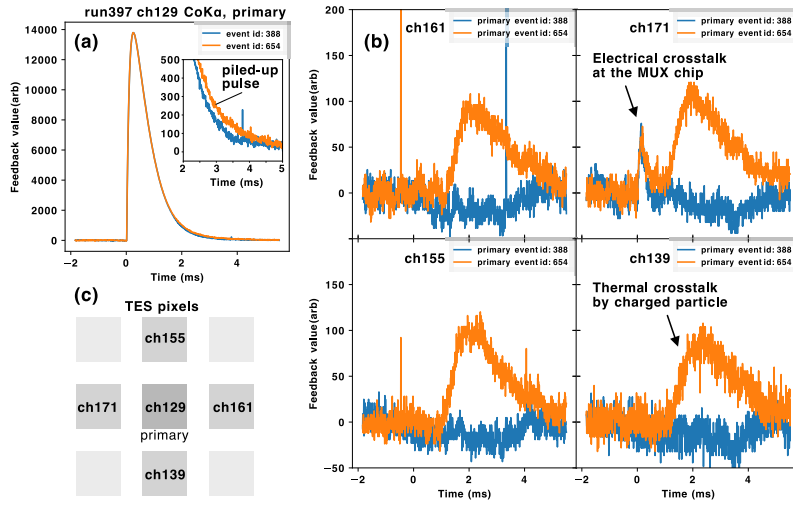


Fig. 1 (a) Co K_{α} X-ray pulses detected by the TES channel 129 (primary record). The inset shows a close-up of the region with thermal crosstalk. (b) Secondary records from the four adjacent TESs taken using the group trigger. The thermal crosstalk is seen in the four adjacent TES channels. The electrical crosstalk seen in the TES channel 171 occurs because the channel 129 and 171 are physically nearest neighbors on the multiplexer chip. (c) The schematic drawing of the TES-pixel positions. (Color figure online.)

pre-trigger crosstalk are removed by applying cuts based on the pre-trigger mean and root-mean-square (rms) values. The application of record length cuts to this region is addressed in section 4.

Thermal crosstalk in the pulse peak region is identified using secondary event records from the four adjacent TES pixels. Here, we define the pulse peak region as 256 samples from the primary trigger (1 sample is $7.2 \mu\text{s}$) and can evaluate the peak-region-mean value (*PRMV*) for each TES except the nearest neighbor channel of the MUX chip to avoid the electrical crosstalk. Abnormally high *PRMV* indicated that an X-ray event is affected by the pulse-peak-region thermal crosstalk. Fig. 2 shows the Co K_{α} X-ray spectra with/without cutting the piled-up events identified by the condition $|PRMV| \geq 10$. The fraction of the number of piled-up events is $\sim 19\%$. The high-energy component of the X-ray peak is excluded by this cut. There is no need for the empirical high-energy tail function to fit the X-ray peaks.

Thermal crosstalk in post peak region (shown in Fig. 1) can be eliminated by reducing record lengths. The results of this technique are shown in Fig. 3, a comparison of a full record-length (1024-sample) analysis to a reduced record-length (524-sample) analysis where 500 samples are discarded at the end. By removing the last 500 samples so that thermal crosstalk in this region won't affect the pulse height determination, the full-width-at-half-maximum (FWHM) energy resolution at the Co K_{α} X-ray energy is improved from 6.6 eV to 5.7 eV and the fraction of the LE tail component is also improved from 28% to 18%. The 18% fraction of the LE tail is same with the data taken in the beam-off condition. This means that no additional LE tail component is needed to fit the X-ray spectra.

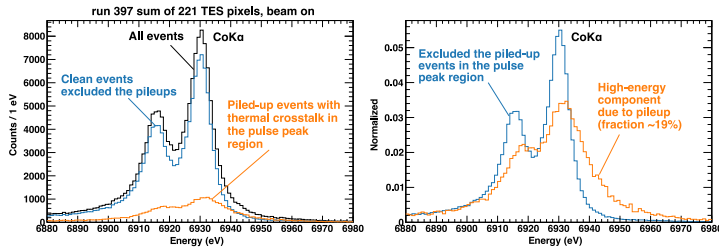


Fig. 2 The beam-on energy spectra of Co K_{α} X-rays summed over 221 TES pixels. *Left*, the energy spectra of all events (*black*), events affected by the thermal crosstalk in the pulse peak region (*orange*), and clean events not affected by the thermal crosstalk in the pulse peak region (*blue*). Events affected by the thermal crosstalk are identified by the condition $|PRMV| \geq 10$ and account for roughly 19 % of all pulse records. *Right*, the normalized spectra of events not affected by thermal crosstalk (*blue*) and affected by thermal crosstalk (*orange*) in the pulse peak region. The orange histogram has a visible high-energy component. (Color figure online.)

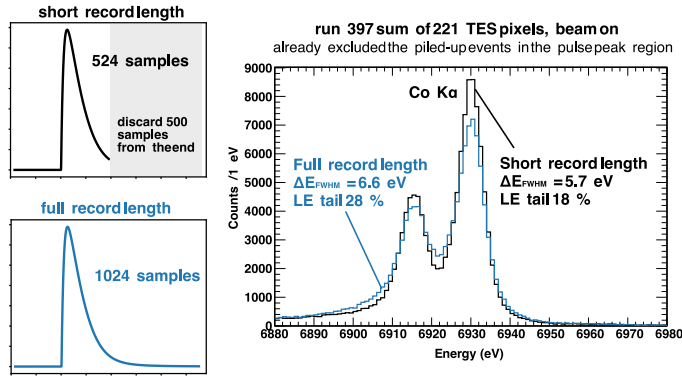


Fig. 3 The effects of shortening record length from 1024 samples to 524 samples. *Left*, the pulse record lengths used for the analysis. *Right*, the Co K_{α} spectra. The use of the shorter record lengths improves the FWHM energy resolution from 6.6 eV to 5.7 eV and reduced the LE tail fraction from 28 % to 18 %.

4 Record Length Dependence

As shown in Fig. 3, the shorter record-length analysis is very useful for the piled-up pulses in the post peak region. It improves not only the energy resolution but also the fraction of LE tail component without losing any event. In order to optimize the record length, we check here the record length dependence of the energy resolution. There are two parameters to shorten the record length, one is the pre-trigger region which changes from the start, the other is the post trigger region which changes from the end. We call the cut for the pre-trigger region as *pre cut* and for the post trigger region as *post cut*. The unit of cut is one point of waveform sampling.

Figure 4 shows the beam-on and beam-off energy resolution at the Co K_{α} X-ray energy as a function of *post cut*. For the beam-on data, the energy resolution improves as *post cut* gets larger, and it becomes minimum around the 500 samples. On the other hand, as *pre cut* gets larger, the energy resolution gets worse. This indicates the pre-trigger region cuts with

pre-trigger mean and rms are enough to get clean pulses, and the baseline evaluation with longer samples is effective to the optimal filtering. For the beam-off data, as both parameters get larger, the energy resolution is degraded. This looks normal for the non-piled-up pulses, because the longer record length is better to reduce the noise contribution [9].

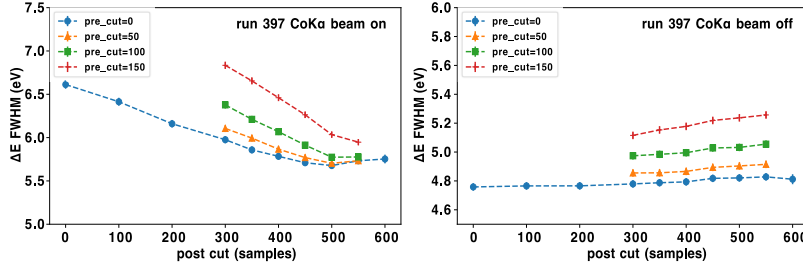


Fig. 4 The record length dependence of the energy resolution at the Co K_{α} X-ray energy as a function of *post cut* samples. *Left*, the beam-on data summed over 221 TES pixels, the markers *circle*, *triangle*, *square*, and *cross* show the different *pre cut* of 0, 50, 100, and 150 samples, respectively. *Right*, the beam-off data. The best resolution is obtained with the *pre cut* = 0, *post cut* = 500 point for the beam-on data. For the beam-off data, the energy resolution is degraded as the record length gets shorter. (Color figure online.)

5 Analysis techniques for energy calibration of beam-on X-ray spectra

As described in the previous sections, the reduction of thermal crosstalk effects enable to eliminate the low-energy and high-energy components. The clean and simple X-ray pulse height spectra are essential to minimize the systematic errors of energy calibration. The energy calibration curve is determined by the X-ray energies and the peak positions obtained by fitting the pulse height spectra. Therefore, it is important to exclude the unexpected components from the pulse height spectra to obtain accurate peak positions. In this section, the analysis methods to be careful about the energy calibration for the beam-on data are summarized.

1. Compute filter with clean pulses. The average pulse should be calculated with the beam-off data to exclude the pileup of thermal crosstalk. If beam-off data are not available, we should select clean pulses with severe conditions.
2. Calibrate the beam-on and beam-off data independently. Use the clean filter of beam-off data, but do not share the calibration curve with beam-on data. The baseline is slightly changing when beam is on in addition to the gain drift, because the heat from the charged particles energy deposits heats the TES pixels. As shown in Fig. 5, the correlation between baseline and pulse height could be slightly off for the beam-on and beam-off data. Therefore the independent energy calibration is desirable for each data set after gain drift correction. In our case, the difference of the X-ray peak position between the beam-on and beam-off data with shared drift correction is about 0.2 eV. Fig. 5 shows the gain drifts for the beam-on and beam-off data and the drift correction for the Co K_{α} X-ray events. The beam-on data show the slightly higher baseline than the beam-off data.
3. Fit with the LE tail function for each X-ray peak if use the thermally evaporated Bi absorbers. The LE tail is an empirical function, the origin is considered as heat traps by

the grain structure of Bi. The fitted peak position without LE tails is off about 0.3 eV in our case.

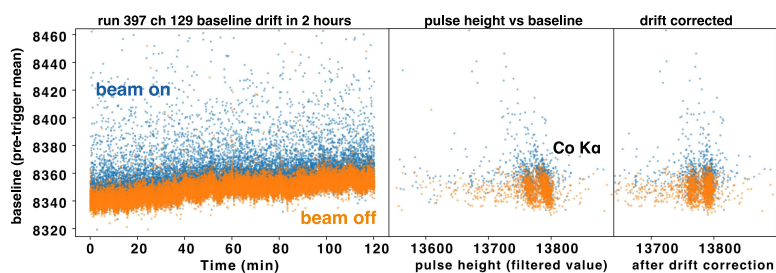


Fig. 5 Gain drift in 2 hours and the drift correction for the beam-on and beam-off data. The beam-on data (*blue*) show the slightly higher baseline and lower pulse height than the beam-off data (*orange*). (Color figure online.)

6 Summary

We have developed the analysis techniques to eliminate the piled-up events with the thermal crosstalk. The high-energy and low-energy components of the X-ray spectra are excluded by using the pulse-peak-region analysis with the group trigger and the shorter record-length analysis to discard the piled-up record timing, respectively. These methods improve the energy resolution from 6.6 eV (FWHM) to 5.7 eV at 6.9 keV and enable simpler fits of X-ray spectra, which leads to precise and accurate energy calibration.

Acknowledgements This work was partly supported by the Grants-in-Aid for Scientific Research (KAKENHI) from MEXT and JSPS (Nos. 16H02190, 15H05438, 18H03714, and 18H05458). We thank the members in the NIST Quantum Sensors Project. We appreciate the significant contributions by J-PARC, RIKEN, and those who kindly have backed up the J-PARC E62 experiment.

References

1. C. Curceanu *et al.*, *Rev. Mod. Phys.* **91**, 025006, (2019), DOI: 10.1103/RevModPhys.91.025006
2. T. Hashimoto *et al.*, *J. Low Temp. Phys.* This Special Issue (2019)
3. S. Okada *et al.*, and the HEATES Collaboration, *Prog. Theor. Exp. Phys.* 091D01, (2016), DOI:10.1093/ptep/ptw130
4. H. Tatsuno *et al.*, and the HEATES Collaboration, *J. Low Temp. Phys.* **184**, 930, (2016), DOI:10.1007/s10909-016-1491-2
5. S. Yamada *et al.*, *J. Low Temp. Phys.* This Special Issue (2019)
6. R. Hayakawa *et al.*, *J. Low Temp. Phys.* This Special Issue (2019)
7. A.E. Szymkowiak, R.L. Kelley, S.H. Moseley, C.K. Stahle, *J. Low Temp. Phys.* **93**, 281, (1993), DOI: 10.1007/BF00693433
8. J.W. Fowler, B.K. Alpert, W.B. Doriese, Y.-I. Joe, G.C. O'Neil, J.N. Ullom, and D.S. Swetz, *J. Low Temp. Phys.* **184**, 374, (2016), DOI: 10.1007/s10909-015-1380-0
9. W.B. Doriese, J.S. Adams, G.C. Hilton, K.D. Irwin, C.A. Kilbourne, F.J. Schima, and J.N. Ullom, *AIP Conference Proceedings* **1185**, 450, (2009), DOI:10.1063/1.3292375